Instruments and techniques

Rates of diffusional exchange between small cells and a measuring patch pipette

Michael Pusch and Erwin Neher

Max-Planck-Institut für biophysikalische Chemie, Am Fassberg, D-3400 Göttingen, Federal Republic of Germany

Abstract. (1) Fluorescent compounds and specific ion currents (Na^+, K^+) were used to study the kinetics of the diffusional exchange between small cells and patch pipettes in the tight seal whole cell configuration of the patch clamp technique. (2) Changes in the intracellular concentration of the test substances following patch rupture could be fitted with single exponentials, provided the access resistance R_A of the pipette remained constant during diffusional equilibration. The diffusion time constants were linearly related to the access resistance. (3) When apparent diffusion rates were normalized with respect to access resistance they were found to be dependent on the cell size. However, the cell capacitance, which is proportional to the membrane area turned out not to be a precise measure of the cell size. (4) The experimental diffusion rates changed systematically with the aqueous diffusion coefficient and the inverse third root of the molecular weight. Linear interpolation with respect to these quantities provided estimates of diffusion time constants for the diffusion between patch pipettes and the cytoplasm for substances of interest.

Key words: Patch clamp — Washout — Cell dialysis — Chromaffin cells

Introduction

The tight seal whole cell configuration of the patch clamp technique provides several means of studying and manipulating small cells. Whole cell currents can be studied with the voltage clamp technique (Hamill et al. 1981), exocytosis can be monitored by measuring the membrane capacitance (Neher and Marty 1982) and changes in intracellular calcium concentration can be measured by loading cells with Ca^{2+}-indicator dyes (Almers and Neher 1985). Unavoidably linked with this technique is a diffusional exchange between pipette and cell. One aspect of this diffusional exchange is the possibility of controlling the cytosolic conditions, which allows the loading of cells with special agents or indicator dyes as discussed by Gomperts and Fernandez (1985). However, the loss of possibly unknown intracellular components may impair the cellular process under investigation. Examples of this effect are the "wash-out" of Ca^{2+}-channels in chromaffin cells (Fenwick et al. 1982) and the "wash-out" of the ability of mast cells to degranulate in response to external stimulation (Lindau

and Fernandez 1986; Penner et al. 1987). Thus, the diffusional exchange introduces ambiguity in interpreting experimental results, because shortly after establishment of the whole cell configuration the cytosolic conditions change with time. On the other hand, studying the time course of a specific wash-out effect may lead to insights into the process under investigation. Diffusional equilibrium between pipette and cell is reached within seconds for small molecules, especially small ions (Marty and Neher 1983). It may take minutes for macromolecules and probably never occurs within the time span of experiments for cell organelles e.g. secretory vesicles. In any case, a quantitative knowledge of the velocity of this diffusional exchange for a wide range of substances is of great importance for all users of the patch clamp technique.

We have measured diffusion time constants for compounds with molecular weights ranging from $23-150,000$ and derived empirical formulas which permit estimates of diffusion time constants depending on molecular size (expressed either by the diffusion coefficient or the molecular weight), on the size of the pipette (expressed by the access resistance) and on the cell size (expressed by cell capacitance, cell radius or cell volume) for arbitrary substances, provided their diffusional behaviour is not markedly disturbed, e.g. by intracellular binding, and provided cells do not have extreme shapes.

Methods

Technique. The measurements were performed in the tight seal whole cell configuration of the patch clamp technique as described by Hamill et al. (1981). Patch pipettes were fabricated from borosilicate glass capillaries (Kimax) with resistance values of $0.5-5\ M\Omega$ when filled with normal saline. Bovine chromaffin cells were prepared as described elsewhere (Marty and Neher 1985). Their size ranged from about $8-15\ \mu m$. They could be used $1-4$ days after preparation. The experiments were performed at room temperature ($21-25°C$).

Whole-cell-currents. The diffusion of Na^+ and K^+ was monitored by measuring Na^+- and K^+-currents respectively, which can easily be separated in chromaffin cells (Fenwick et al. 1982; Marty and Neher 1985). The bath solution contained (in mM) 140 NaCl, 2.8 KCl, 10 $CoCl_2$, 2 $MgCl_2$, 10 HEPES-NaOH, 5 glucose, pH 7.2. Co^{2+} was added in order to block Ca^{2+}-channels. Na^+-currents were supressed by ca. 5 μM tetrodotoxin (TTX) when measuring K^+-currents. The pipette solution for monitoring Na^+-dif-

fusion was a Na^+-rich solution containing 100 NaCl, 40 CsCl, 10 HEPES-NaOH, 10 EGTA, pH 7.2. Cs^+ was used to suppress K^+-currents. For measuring K^+-currents, a K^+-deficient pipette solution was used containing 140 tetramethylammonium (TMA)Cl, 2 $MgCl_2$, 10 HEPES-KOH, 10 EGTA, pH 7.2. TMA was used as an "inert" cation which should not be permeable through K^+-channels but which also should not block them.

After obtaining a gigaseal, depolarizing voltage pulses to 30−40 mV (4 ms long for Na^+-currents and 40 ms long for K^+-currents) were applied at a rate of 2 Hz from a holding potential of −80 mV. Then suction was applied to the pipette in order to establish the whole cell configuration. Currents were recorded during equilibration of Na^+- and K^+-concentration respectively. The records were filtered at 10 kHz (Na^+) and 2.5 kHz (K^+) respectively, sampled, and stored on a PDP 11/73 laboratory computer. The slow transient cancellation of the EPC-7 patch clamp amplifier could not be adjusted properly, because the currents had to be recorded immediately after patch rupture. However a P/4-method (Bezanilla and Armstrong 1977) allowed for compensation of leak current. After completion of diffusion the slow transient cancellation was adjusted and the values of access conductance and cell capacitance were read from the EPC-7 potentiometers. Inactivation of Na^+-currents due to the fast rate of depolarizations was found not to be significant in control experiments.

In order to reconstruct the time course of the intracellular Na^+-or K^+-concentration from the current records, it was assumed, that the current amplitude at a specific time after a depolarizing pulse is linearly related to the momentary intracellular ion concentration. This assumption is supported by the Goldman-Hodgkin-Katz current equation for one permeable ion:

$$I = zFP\Psi \frac{c_i e^\Psi - c_o}{e^\Psi - 1}, \tag{1}$$

where $\Psi = ZFU/RT$ and U is the membrane potential; c_i and c_o are the intracellular and extracellular concentrations respectively. Activation and inactivation processes are described by the time dependent factor P. The linearity between current and concentration at a given potential was verified by comparing currents obtained with different pipette solutions (see Results). The mean value of the current over a certain time after depolarization (which for short will be called 'current amplitude' and represents roughly the peak current in the case of Na^+-currents and the steady state current in the case of K^+-currents) was considered to represent the momentary intracellular ion concentration. A single exponential of the form

$$I(t) = I_\infty - I_1 \exp(-t/\tau), \tag{2}$$

where t is the time of the depolarizing pulse after establishment of the whole cell configuration and $I(t)$ is the current amplitude, was fitted to the data points by the least squares method yielding the diffusion time constant τ.

Fluorescence and lock-in measurements. The diffusion of fluorescence-labeled substances was monitored by measuring the increase of fluorescence of the cell after patch rupture employing a Zeiss IM35 microscope, equipped with epifluorescence, a xenon-arc lamp, a filter set depending on the substance in use, and a photomultiplier (Zeiss, photometer SF). Light was collected from a circular area of ∼20 μm
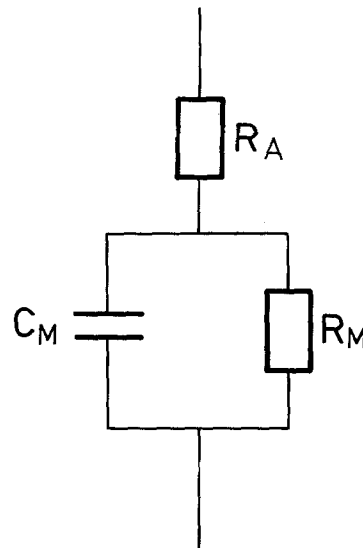

Fig. 1. Simplified equivalent circuit for the tight seal whole cell configuration. Seal resistance (shunt) and stray capacitance are neglected for simplicity

diameter, where the cell under investigation had been placed. The photomultiplier analog signal was fed to the analogue to digital converter of a PDP 11/73 laboratory computer. The access conductance of the pipette and the cell capacitance, which both are important parameters for diffusional exchange (see below), were measured simultanously with the fluorescence signal using a 2-phase lock-in amplifier as described by Lindau and Neher (1988). Briefly, the electrical admittance of the cell-pipette-configuration was measured at 800 Hz by adding a sinusoidal voltage (16 mV rms) to the command potential and measuring the resulting sinusoidal current at two mutual orthogonal phase angles. Together with the applied DC-potential and the DC-current (after filtering out the sinusoidal component) the two lock-in-signals (real and imaginary part of the admittance) were digitized and fed to a PDP 11/73 laboratory computer. Offsets resulting from the pipette capacitance were canceled during the cell-attached configuration before penetrating the cell.

All signals (including fluorescence) were averaged over at least 0.1 s and stored; subsets were displayed on-line on a vector display. Later the access conductance and the cell capacitance were calculated based on the equivalent circuit shown in Fig. 1. The admittance of this network is given by

$$Y(\omega) = A + iB = \frac{1 + i\omega C_M R_M}{R_A + R_M + i\omega C_m R_M R_A}. \tag{3}$$

From A and B and the DC-conductance b, which is given by

$$b = \frac{1}{R_A + R_M}, \tag{4}$$

the three parameters R_A, C_M and R_M can be calculated using the equations

$$R_A = \frac{A - b}{A^2 + B^2 - Ab}, \tag{5}$$

$$C_M = \frac{1}{\omega B} \frac{(A^2 + B^2 - Ab)^2}{(A - b)^2 + B^2} \qquad (6)$$

and

$$R_M = \frac{1}{b} \frac{(A - b)^2 + B^2}{A^2 + B^2 - Ab} . \qquad (7)$$

(see Appendix for a derivation of these equations).

The analysis of the fluorescence experiments was impeded by two difficulties: The access conductance $G_A = 1/R_A$ usually did not remain constant in the course of most experiments. As a consequence the time course of the fluorescence increase was nonexponential. The second problem arose from significant bleaching of some fluorescence dyes, which disturbed diffusion kinetics. Both problems can be accounted for with some reasonable assumptions. In the simplest case, when bleaching is not significant and the access conductane remains constant, the time course of fluorescence can be described by a simple differential equation:

$$\frac{d(c - c_0)}{dt} = -\frac{1}{\tau}(c - c_0), \qquad (8)$$

where c is the intracellular concentration at time t and c_0 is the constant concentration inside the pipette. This expression is based on the assumption that the diffusion process is rate-limited by the diffusion through the relatively small opening of the pipette tip, implying that the concentrations inside the cell and inside the pipette are approximately homogeneous. Equation (8) has the solution

$$c(t) = c_0 - c_1 \exp(-t/\tau), \qquad (9)$$

where c_1 is determined by $c(0) = c_0 - c_1$. The access conductance G_A in the whole cell configuration is not identical with the conductance of the pipette immersed in the bath (Marty and Neher 1983). Here we always refer to the access conductance during the whole cell configuration G_A, which may change with time. We assume equivalence of electrical and diffusional mobility for the major current carriers which means that geometrical factors, such as the shape of the pipette and the area of the tip opening, are faithfully reflected by access conductance. Thus changes of the access conductance can be included into this description, if one assumes that the rate of change of the intracellular concentration at a given time is proportional to the momentary access conductance G_A as is actually observed (see Results section). Equation (8) can then be transformed to

$$\frac{d(c - c_0)}{dt} = -k \cdot G_A(t) \cdot (c - c_0). \qquad (10)$$

For constant access conductance G_A the "normalized diffusion rate" k is given by

$$k = \frac{1}{G_A \tau}. \qquad (11)$$

This quantity is an 'apparent rate' since it also includes the effects of cell volume and geometry. Equation (10) has the solution

$$c(t) = c_0 - c_1 \exp[-k \cdot H(t)], \qquad (12)$$

with $H(t) = \int_0^t G_A(t')dt'$.

If one assumes, that the decrease in fluorescence caused by bleaching is proportional to the momentary intracellular

Table 1. Table of properties and measured diffusion rates of all substances used

Substance	M	D in 10^{-11} $m^2 s^{-1}$	k in $10^4 \, \Omega s^{-1}$	$k \cdot C_M^{1.5}$ in $10^{-14} \, \Omega F^{1.5} s^{-1}$
Na$^+$	23	131	132 $\pm$ 41	1966 $\pm$ 831
K$^+$	39	187	261 $\pm$ 191	3450 $\pm$ 1560
FD4	4100	9.55	8.57$\pm$ 2.7	122 $\pm$ 44
FD10	9000	8.63	3.80$\pm$ 1.3	51.9$\pm$ 18.7
FD40	42000	5.97	5.28$\pm$ 2.8	68.6$\pm$ 44.2
FD70	71000	4.69	1.54$\pm$ 0.66	20.6$\pm$ 8.7
FD150	156000	2.33	1.80$\pm$ 0.80	30.7$\pm$ 17.1
Peroxidase	40500	7.05	2.50$\pm$ 1.38	29.7$\pm$ 19.6
IgG	150000	4.0	2.63$\pm$ 1.77	33.1$\pm$ 21.3
Fura-2	637	50	22.7 $\pm$ 3.8	377 $\pm$ 64
F-c-AMP	748	37.5*	36.8 $\pm$ 3.5	460 $\pm$ 64
F-c-GMP	748	37.5*	17.1 $\pm$ 6.9	164 $\pm$ 44
Glu-LRB	688	38.8*	5.94$\pm$ 2.21	113 $\pm$ 50
Pyranine	405	48.1*	10.4 $\pm$ 5.6	191 $\pm$ 131
Phallacidin	1070	32.5*	1.97$\pm$ 1.5	14.3$\pm$ 8.9

First column: name of the substance, *second column:* molecular weight, *third column:* diffusion coefficient (* indicates that the value was estimated), *fourth column:* 'normalized diffusion rate' k, *fifth column:* 'normalized diffusion rate $k \cdot C_M^{1.5}$ (see Methods for the meaning of k and $k \cdot C_M^{1.5}$)

concentration, Eq. (10) is changed by adding a term that is proportional to c:

$$\frac{dc}{dt} = k \cdot G_A(t) \cdot (c_0 - c) - k_B \cdot c, \qquad (13)$$

where k_B is the bleaching rate, which depends mainly on the intensity of the exciting light. Equation (13) has the solution

$$c(t) = c_0[1 - W(t) \exp(-kH(t) - k_B t)] - c_1$$
$$\exp(-kH(t) - k_B t), \qquad (14)$$

where $H(t)$ is as above and

$$W(t) = k_B \int_0^t \exp[kH(s) + k_B s]ds .$$

The experimental time courses were analysed by fitting a function of the form (12) or of the form (14) (depending on whether bleaching was significant or not) to the data points. The parameters c_0, c_1 and k were determined using the least squares method. The bleaching rate k_B was determined in separate experiments.

The substances. The substances used are listed in Table 1 together with the corresponding diffusion coefficients and molecular weights. In some cases the diffusion coefficient for aqueous diffusion could not be found in the literature. In these cases an empirical interpolating formula for low molecular weight substances derived by Longsworth (1952, 1953) was applied to estimate the diffusion coefficient. The substances were dissolved in a pipette solution containing (in mM) KCl, 140; KOH-EGTA, 10; HEPES-KOH, 10; MgCl$_2$, 2; pH 7.2.

The diffusion coefficients for Na$^+$ and K$^+$ were taken from Landoldt-Börnstein (1969) for aqueous solutions of ca. 100 mM Nacl and KCl respectively.

FD4, FD10, FD40, FD70 and FD150 are dextrans labeled with FITC (Sigma, St. Louis, MO, USA). Since dextrans are polymolecular substances, the molecular

weights are mean values. In order to get more homogeneous samples, the dextrans were purified by gel-filtration using Sephacryl S-400 Superfine gels (Pharmacia, Uppsala, Sweden). Fractions (ca. 2 ml) were taken every $1-2$ min and the three fractions with highest absorption at 490 nm were further used. The diffusion coefficients were taken from Callaghan and Pinder (1983). Since the dextrans from Callaghan and Pinder did not have the same molecular weights as those used here, their values were interpolated. The values were linearly correlated with respect to $M^{-1/3}$.

The diffusion coefficient and molecular weight of FITC-labeled peroxidase (Sigma) was taken from Cecil and Ogston (1951).

FITC-labeled IgG was kindly provided by Dr. J. Wehland. Diffusion coefficient and molecular weight were taken from the Handbook of Biochemistry (1976). Since gigaseals were difficult to obtain with IgG or peroxidase in the pipette, the concentrations of these proteins had to be kept low which increased the noise in the fluorescence recordings.

NBD-phallacidin (Molecular Probes, Eugene, OR, USA) has spectral properties similar to FITC and is normally used for staining the actin-cytoskeleton (Barak et al. 1980). Thus, it is expected that NBD-phallacidin exhibits pronounced intracellular binding. The diffusion coefficient was estimated (see above).

For all FITC-labeled compounds the Zeiss-FITC fluorescence filter set could be used (transmitting filter 485 $\pm$ 10 nm, dichroic mirror 510 nm, barrier filter 540 $\pm$ 20 nm).

Fura-2 is a Ca^{2+}-indicator dye. The diffusion coefficient is taken from Timmerman and Ashley (1986). Fluorescence was measured as described by Almers and Neher (1985).

The amino acid glutamine labeled with lissamine-rhodamine-B (Glu-LRB) was kindly provided by Dr. W. Loewenstein. Its diffusion coefficient was estimated. The fluorescence was monitored using the rhodamine filter set of Zeiss (transmitting filter 546 $\pm$ 6 nm, dichroic mirror 580 nm, barrier filter 590 nm).

The pH-indicator dye pyranine (Serva, Heidelberg, FRG) was kindly provided by Dr. R. Uhl. The diffusion coefficient was estimated. The spectral properties are described by Kano and Fendler (1978). The fluorescence could be measured with the same filters as for Fura-2 (leaving out the first UV interference filter).

Fluorescence of cyclic AMP and cyclic GMP labeled with a substance similar to fluorescein (substances F-1039 and F-1041 from Molecular probes, here called F-c-AMP and F-c-GMP) could be observed with the FITC filter set. Diffusion coefficients were estimated.

Results

The assumption that the "current-amplitude" is linearly related to the intracellular ion concentration was tested for Na^+- and K^+-currents with four different pipette solutions each containing Na^+ and K^+-concentrations ranging from $0-90$ mM and from $0-140$ mM respectively. The currents were recorded after completion of the diffusional exchange. Cells were impaled multiply in order to eliminate cell to cell variations. ('Rundown' of the currents due to the multiple impalement was found to be small compared to the dependence on the ionic concentrations.) It was found that the current amplitude was linearly related with the ion concen-

tration for depolarizing voltages not greater than $40-60$ mV. (The deviations from linearity were smaller than the scatter between individual measurements.)

Bleaching of fluorescence dyes was examined by loading cells with the dye via a patch pipette and then pulling back the pipette which normally resulted in the outside-out configuration of the patch clamp technique. The cell membrane usually resealed at the point were the pipette was attached before. The following exponential decrease in fluorescence was interpreted as being caused by bleaching. This interpretation was confirmed by the observation that the fluorescence did not decrease if the exciting light was switched off for a certain time period. Bleaching was found to be significant only for substances labeled with FITC with a common bleaching time constant (for the selected intensity of the exciting light) of

$$\tau_B = 590 \text{ s}.$$

This time constant was taken into account according to Eq. (14) for substances labeled with FITC.

In order to confirm the assumption that the diffusion rate is proportional to the access conductance, which underlies the analysis method in the case of nonconstant access conductance, we selected experiments during which the access conductance remained relatively constant and plotted the inverse diffusion time constant τ versus access conductance G_A. Figure 2 shows an example for the dextran FD70. In spite of a large scatter it can be seen that there is a definite positive correlation (correlation coefficient = 0.845 in this case). The correlation between diffusion rate and access conductance was similar for the other substances.

Another way of testing linearity is to test whether the experimental time courses can be described by Eq. (14) in the case of variable access conductance. It turned out, that in nearly all cases the experimental time courses could well be described by Eq. (14). Figure 3 shows as examples two typical experiments, in which the upper traces represent the fluorescence change after patch rupture and the lower traces the corresponding access conductance G_A. The dotted lines, which partially overlap with the original traces represent fits according to Eq. (14). It can be seen, that the decrease in fluorescence in B, which is probably due to impeded replenishment after decreased G_A, can be well described by Eqn. (14). The relative deviation of the fits from the experimental time courses, which is defined by

$$\Delta = \frac{\int [y_1(t) - y_2(t)]^2 dt}{\sqrt{\int y_1^2(t) dt \cdot \int y_2^2(t) dt}}$$

for two functions y_1 and y_2, ranged from 10^{-5} to 10^{-8}.

The normalized diffusion rate k [see Eq. (13)] should be dependent on the cell size. More precisely one expects that the diffusion rate is proportional to the inverse cell volume. Since for spherical cells the cell volume is proportional to $area^{1.5}$ and the electrical capacitance C_M is proportional to the area one expects that the diffusion rate is proportional to $C_M^{-1.5}$. Figure 4 shows a double logarithmic plot of the normalized diffusion rate k versus cell capacitance C_M for Fura-2. There is a large scatter and the slope in this case is -0.7 instead of the expected -1.5. The slope varied between -0.6 and -2.2 for the different substances. Thus the correlation between cell capacitance and diffusion rate is quite loose. However in order to extrapolate the results presented here to larger or smaller cells, it is reasonable to scale them according to the cell volume.
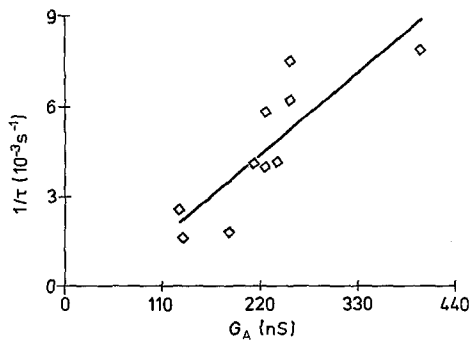
Fig. 2. Inverse diffusion time constant τ^{-1} versus access conductance G_A for selected experiments during which the access conductance remained constant. (Substance FD70, correlation coefficient $r = 0.854$)
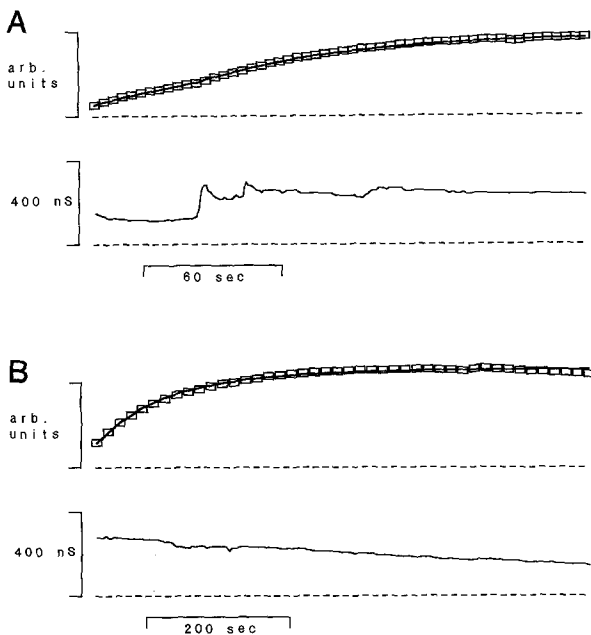

Fig. 4. Double-logarithmic plot of the normalized diffusion rate k versus cell capacitance C_M for Fura-2. The *regression line* has a slope of -0.7 (correlation coefficient $r = -0.71$)

Fig. 3A, B. Typical experimental fluorescence changes after patch rupture (*upper trace*) and corresponding access conductance (*lower trace*). The symbols in the *upper trace* represent data points (not all points shown for clarity), the *solid lines* in the *upper trace* represent fits according to Eq. (14) ($\tau_B = 590$ s). Substance in **A**: FD10 (ca. 5 mg/ml), normalized diffusion rate k from the fit $k = 5.74 \cdot 10^4\ \Omega s^{-1}$; substance in **B**: FITC-labeled peroxidase (ca. 0.5 mg/ml), $k = 3.0 \cdot 10^4\ \Omega s^{-1}$

Fig. 5. Double-logarithmic plot of the mean normalized diffusion rate k versus diffusion coefficient D for all substances. The slope of the regression line is 1.06 (correlation coefficient $r = 0.92$). The value of NBD-phallacidin is not included in the regression

Table 1 lists all experimental results. For each substance at least 25 experiments were performed.

The first column contains the name of the substance (see 'Methods' for more information concerning the substances), the second column lists the molecular weight and the third column contains the diffusion coefficient for aqueous diffusion. An asterisk indicates that the corresponding coefficient could not be found in the literature and that it was estimated using an empirical formula derived by Longsworth (1952, 1953). The fourth column lists the averaged normalized diffusion rate k and the last column contains the averaged diffusion rate normalized also with respect to cell capacitance. The errors are standard deviations.

It is expected that the diffusion rate k is proportional to the diffusion coefficient D. Figure 5 shows a double-
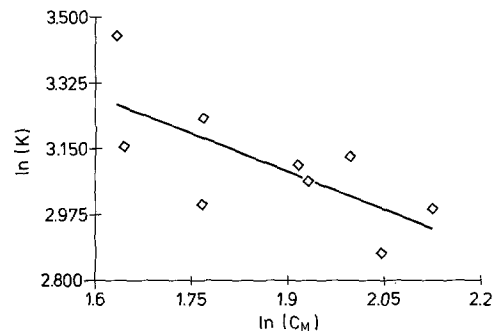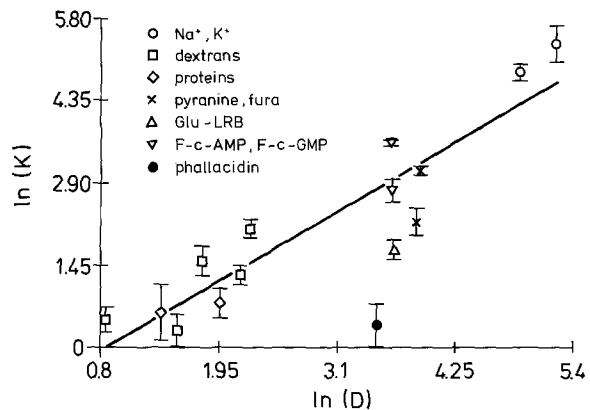
logarithmic plot of the diffusion rate k versus the diffusion coefficient D. Linear regression gives a slope of 1.06, which is in accordance with the theoretical expectation. Nevertheless there is a large scatter of the data points. The data point corresponding to NBD-phallacidin was not included in the linear regression because it is much smaller than all the other values with comparable molecular weight. This is probably due to strong intracellular binding to the actin cytoskeleton of the cell. The large scatter may partly be due to unprecise values of the diffusion coefficients especially for the polymolecular dextrans and some low molecular weight substances.

Since for larger molecules approximately $D \propto M^{-1/3}$, a linear correlation of k with $M^{-1/3}$ is therefore expected. Figure 6 shows a double-logarithmic plot of the diffusion rate k versus molecular weight. Here the values of Na^+ and K^+ are excluded because the relation $D \propto M^{-1/3}$ certainly does not hold for small ions. The regression line has a slope of -0.41. This is different from the theoretical expectation of $-1/3$, but it can be seen that the dashed line which has a slope of $-1/3$ approximates the data points almost equally well.

In order to derive empirical interpolating formulas, the diffusion rate k was linearly related with D and $M^{-1/3}$ respectively. The scatter in these linear plots is still higher
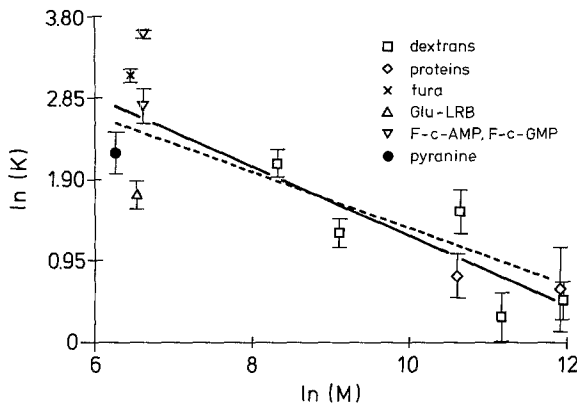
Fig. 6. Double-logarithmic plot of the mean normalized diffusion rate k versus molecular weight for all substances except Na^+, K^+ and NBD-phallacidin. The solid regression line has a slope of -0.41 (correlation coefficient $r = -0.87$), the *dotted line* is shown for comparison and has a slope of $-1/3$

Fig. 7. Normalized diffusion rate $k \cdot C_M^{1.5}$ for F-c-AMP (●) and F-c-GMP (■) at different pipette concentrations

than in the double-logarithmic plots (not shown). By linear regression one obtains the following equations. [The errors are purely statistical errors and do not include the errors of the individual data points (Walcher 1971).]

$$\frac{k}{10^4\,\Omega s^{-1}} = (1.28 \pm 0.11) \cdot \frac{D}{10^{-11}\,m^2\,s^{-1}} - (14.5 \pm 6.9)$$

(15)

$$\frac{k}{10^4\,\Omega s^{-1}} = (166 \pm 48)M^{-1/3} - (1.1 \pm 3.6).$$

(16)

These equations are valid only for cells of a size comparable to that of chromaffin cells. The mean capacitance of the cells was

$$C_0 = (5.91 \pm 1.95)pF \quad (n = 397).$$

In order to relate this electrical parameter to the geometrical size, the radius and capacitance of a series of cells was measured, and the following relation was obtained:

$$\frac{C_M}{pF} = (0.105 \pm 0.015)\left(\frac{r}{\mu m}\right)^2 - (0.3 \pm 0.8).$$

Therefore the mean capacitance of $C_0 \pm 5.91$ pF corresponds to a mean radius of $r_0 = 7.68$ μm. With the formula $V = 4\pi r^3/3$ this corresponds to a volume of $V_0 = 1897\,(\mu m)^3$.

Equations (15) and (16) represent the diffusion properties of the bulk of substances tested. However two abnormalities were observed. Firstly, NBD-phallacidin diffused much slower than expected probably due to binding, as mentioned above. Secondly, the diffusion rates of F-c-AMP and F-c-GMP turned out to be concentration dependent. At lower concentrations the diffusion was considerably slower than expected. This is shown in Fig. 7. In this plot the normalized diffusion rate $k \cdot C_M^{1.5}$ is plotted versus the logarithm of the concentration of the dye in the pipette for F-c-AMP (three concentrations) and F-c-GMP (two concentrations). The slower diffusion at lower concentration might be due to saturable intracellular binding, since the binding should be less significant at higher concentration. Inconsistent with this hypothesis is the nonsaturating behaviour of the 3 data points for F-c-AMP. However, it was not possible
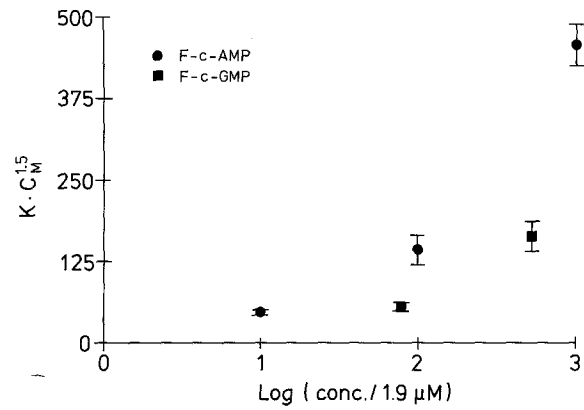
to examine if saturation occurs at higher concentration because of the low solubility of F-c-AMP and F-c-GMP (ca. $1-5$ mM). Another explanation for the dependence on concentration could be fluorescence quenching at higher concentration which would also lead to an apparent higher diffusion rate. Two facts argue against this hypothesis. At first, the absolute fluorescence intensity was roughly proportional to the concentration of the dye in the pipette, and secondly the values for the diffusion rate at high concentrations is comparable to the value for Fura-2, which has similar molecular weight and the diffusion rate of which is not dependent on concentration. Both arguments are not compatible with fluorescence quenching. In order to avoid the effect of concentration dependence as best as possible, only the values at the highest concentration were taken for the interpolation formula.

Discussion

Measurement of the diffusional exchange rates between patch pipette and adrenal chromaffin cells shows that there is a correlation between the loading time course of a given pipette-cell assembly and its electrical parameters, access resistance (indicative of the size of the cell-pipette connection) and membrane capacitance (indicative of cell size). Also, comparing the diffusional properties of 15 different substances, it is clear that there is a strong correlation between the loading time constant and the molecular weight (or the aqueous diffusion coefficient) of the diffusing substance. Unfortunately there is a large scatter in the experimental data. Reasons for this scatter can be sought in retarded diffusion due to binding, and in geometrical factors. Especially the relatively poor correlation of the diffusion rate with the cell capacitance can be explained by variations of the freely accessible cell volume caused e.g. by different sizes of the nucleus or by different contents of secretory granules. Also the shape of the outer membrane is certainly different from a smooth, mathematically ideal sphere. Thus the membrane area expressed by the cell capacitance may not be a good measure for the cell volume.

The scatter of the data points in Figs. 5 and 6 is probably partially due to uncertain diffusion coefficients. Errors in the estimation of diffusion coefficients can be expected in the case of the dextrans, which are heterogenous substances, and in the case of those low molecular weight substances

for which no diffusion coefficient could be found in the literature. Another reason for the scatter may be different intracellular binding properties of the different substances. That intracellular binding may alter the apparent diffusion velocity significantly, is exemplified by NBD-phallacidin, which shows a very slow apparent diffusion due to affinity for intracellular proteins. The slower diffusion of dyes and ions inside the cytoplasm has been reported for several substances. The diffusion of Fura-2 in cytoplasm of muscle cells is about ten times slower than in aqueous solution (Timmerman and Ashley 1986). Connor and Ahmed (1984) report, that the indicator dyes phenol red and arsenazo III diffuses five times slower in neuronal cytoplasm, that Ba^{2+} and H^+ diffuse slow compared with aqueous diffusion, and that the diffusion of Ca^+ is restricted by intracellular buffering. These irregular diffusive behaviours of different substances may also explain the large scatter of the data obtained here.

In spite of the scatter, the interpolations of Eqs. (15) and (16) can be utilized as order of magnitude estimates for the diffusional properties of substances for which either the diffusion coefficient or the molecular weight is known. Neglecting intersections with the k-axis in Eqs. (15) and (16), which are uncertain anyway, the results can be expressed in terms of time constants τ, as functions of diffusion coefficient D or molecular weight M:

$$\tau = (78.4 \pm 6.6) \cdot \frac{R_A}{D}, \tag{17}$$

$$\tau = (0.60 \pm 0.17) \cdot R_A \cdot M^{1/3}, \tag{18}$$

where τ is in seconds, R_A is in MΩ, D is in 10^{-7} cm^2 s^{-1} and M is in daltons. It should be noted that these time constants have to be modified if cells differ in size or geometry from our 'standard' chromaffin cell. Our cells have a mean capacitance of

$$C_0 = 5.91 \text{ pF},$$

a mean radius of

$$r_0 = 7.68 \text{ μm},$$

which, assuming spherical geometry, would result in a mean volume of

$$V_0 = 1897 \ (\mu\text{m})^3.$$

In order to apply the formulas to cells of different size, the diffusion time constants should be scaled by the volume:

$$\frac{\tau}{\tau_0} = \frac{V}{V_0}$$

with τ_0 calculated by Eqs. (17) or (18). This scaling may not meet the conditions found in cells with complex geometry, e.g. nerve fibers. For spherical cells one may scale the diffusion time constant using the cell radius or the cell capacitance:

$$\frac{\tau}{\tau_0} = \left(\frac{r}{r_0}\right)^3,$$

$$\frac{\tau}{\tau_0} = \left(\frac{C_M}{C_0}\right)^{1.5}.$$

It should be pointed out that these are empirical formulas based on a limited selection of substances including proteins, dextrans, nucleotides, indicator dyes and small ions. As can be seen in Figs. 6 and 7, the diffusive behaviour does not show a marked dependence on the class of the substance (e.g. dextrans diffuse roughly as fast as proteins of comparable size).

The slow diffusion of NBD-phallacidin and F-c-AMP and F-c-GMP at low concentrations show that significant deviations from the interpolation formulas are possible, especially at low concentrations, if the diffusing substance exhibits significant extracellular binding.

The only molecular parameters appearing in Eqs. (17) and (18) are the aqueous diffusion coefficient and the molecular weight. Possible effects of the electrical charge of the diffusing molecule on the diffusion velocity are only partially grasped by Eq. (17), which uses the aqueous diffusion coefficient, and are totally ignored by Eq. (18). Effects of the charge on the diffusive behaviour strongly depend on the ionic strength of the solution. On the one hand they arise from the electrophoretic effect and on the other hand are due to diffusion potentials (Bockris and Reddy 1977, p. 431 and p. 418). A simple mathematical treatment of the electrophoretic effect (Bockris and Reddy 1977, p. 431) provides a relation between the diffusion coefficient and the ionic concentrations:

$$D = D_\infty \left(1 - \frac{\kappa \omega e_0^2}{6 \ \varepsilon k T}\right),$$

where D_∞ is the diffusion coefficient at infinite dilution, κ the inverse Debye-length, e_0 the elementary charge, ε the dielectric constant of the solution, k the Boltzmann-constant, T the temperature and ω a numerical factor of the order 1 depending on the ionic composition. For a 150 mM solution of univalent ions the term $\kappa \omega e_0^2/(6 \ \varepsilon k T)$ has a value of 12% such that influences of the charge on the diffusive behaviour are confined to the "10-percent-range".

In this study we have measured mainly the diffusion velocity of certain substances from the pipette into the cell. The results should, however, be equally applicable for estimating time constants for the dilution of cellular substances into the pipette (Penner et al. 1987) as long as the diffusion is not disturbed e.g. by intracellular binding.

Appendix: Derivation of the "equivalent-circuit-equations".

The admittance of the network shown in Fig. 1 is given in Eq. (3). Using the abbreviations

$$b = \frac{1}{R_A + R_M},$$

which is the DC-conductance, and

$$A = Re(Y), \ B = Im(Y), \ x = \omega C_M R_M, \ a = R_A b,$$

the admittance can be written as

$$A = b \frac{1 + x^2 a}{1 + x^2 a^2}, \tag{A1}$$

$$B = bx \frac{1-a}{1+x^2 a^2} \, . \tag{A2}$$

Solving (A1) for x^2 yields

$$x^2 = \frac{b-A}{a(Aa-b)} \, . \tag{A3}$$

Hence

$$1 + a^2 x^2 = \frac{b(a-1)}{Aa-b} \, .$$

Inserting this into Eq. (A2) gives

$$B = x(b - Aa) \, . \tag{A4}$$

Squaring this equation, inserting the expression for x^2 and solving for a yields

$$a = bR_A = b \frac{A-b}{A^2 + B^2 - Ab} \, . \tag{A5}$$

Thus

$$R_A = \frac{A-b}{A^2 + B^2 - Ab} \, .$$

From the definition of b it follows that

$$R_M = \frac{1}{b} - R_A = \frac{1}{b} \frac{(A-b)^2 + B^2}{A^2 + B^2 - Ab} \, . \tag{A6}$$

Substituting the expression for $Aa - b$ resulting from Eq. (A4) into Eq. (A3) gives

$$x = \frac{A-b}{Ba} = \omega C_M R_M \, .$$

Hence

$$C_M = \frac{1}{\omega R_M} \frac{A-b}{Ba} \, .$$

Inserting the equations for R_M (A6) and a (A5) finally gives

$$C_M = \frac{1}{\omega B} \frac{(A^2 + B^2 - Ab)^2}{(A-b)^2 + b^2} \, .$$

References

Almers W, Neher E (1985) The Ca signal from fura-2 loaded mast cells depends strongly on the method of dye-loading. FEBS Lett 192:13—18

Barak LS, Yocum RR, Nothnagel EA, Webb WW (1980) Fluorescence staining of the actin cytoskeleton in living cells with 7-nitrobenz-2-oxa-1,3-diazole-phallacidin. Proc Natl Acad Sci USA 77:980—984

Bezanilla F, Armstrong M (1977) Inactivation of the sodium channel. J Gen Physiol 70:549—566

Bockris JO'M, Reddy AKN (1977) Modern electrochemistry, vol 1. Plenum Press, New York

Callaghan PT, Pinder DN (1983) A pulsed field gradient NMR study of self-diffusion in a polydisperse polymer system: dextran in water. Macromolecules 15:968—973

Celcil R, Ogston AG (1951) Determination of sedimentation and diffusion constants of horse-radish peroxidase. Biochem J 49:105—106

Connor JA, Ahmed Z (1984) Diffusion of ions and indicator dyes in neural cytoplasm. Cell Mol Neurobiol 4:53—66

Fenwick EM, Marty A, Neher E (1982) Sodium and calcium channels in bovine chromaffin cells. J Physiol 331:599—635

Gomperts BD, Fernandez JM (1985) Techniques for membrane permeabilization. TIB: 414—417

Hamill OP, Marty A, Neher E, Sakmann B, Sigworth FJ (1981) Improved patch-clamp techniques for high-resolution current recording from cells and cell-free membrane patches. Pflügers Arch 391:85—100

Handbook of biochemistry and molecular biology: Proteins, volume II (1976) Fasman GD (ed), 3rd edn. CRC Press, Cleveland, p 249

Kano K, Fendler JH (1978) Pyranine as a sensitive pH probe for liposome interiors and surfaces, pH gradients across phospholipid vesicles. Biochim Biophys Acta 509:289—299

Landoldt-Börnstein (1969) Zahlenwerte und Funktionen. Vol 2, no. 6, Schäfer K (ed). Springer, Berlin Heidelberg New York, pp 616—621

Lindau M, Fernandez JM (1986) IgE-mediated degranulation of mast cells does not require opening of ion channels. Nature 319:150—153

Lindau M, Neher E (1988) Patch-clamp techniques for time-resolved capacitance measurements in single cells. Pflügers Arch 411:137—146

Longsworth, LG (1952) Diffusion measurements, at 1°, of aqueous solutions of amino acids, peptides and sugars. J Am Chem Soc 74: 4155—4159

Longsworth LG (1953) Diffusion measurements, at 25°, of aqueous solutions of amino acids, peptides and sugars. J Am Chem Soc 75:5705—5709

Marty A, Neher E (1983) Tight-seal whole-cell recording. In: Sakmann B, Neher E (eds) Single channel recording. Plenum Press, New York, pp 107—122

Marty A, Neher E (1985) Potassium channels in cultured bovine adrenal chromaffin cells. J Physiol 367:117—141

Neher E, Marty A (1982) Discrete changes of cell membrane capacitance observed under conditions of enhanced secretion in bovine adrenal chromaffin cells. Proc Natl Acad Sci USA 79:6712—6716

Penner R, Pusch M, Neher E (1987) Washout phenomena in dialysed mast cells allows discrimination of different steps in stimulus-secretion coupling. Bioscience Reports (in press)

Timmerman MP, Ashley CC (1986) Fura-2 diffusion and its use as an indicator of transient free calcium changes in single striated muscle cells. FEBS Lett 209:1—8

Walcher W (1971) Praktikum der Physik, 2nd edn. Teubner, Stuttgart, pp 31—33